ASTROCHEMISTRY

Liquid-like behavior of UV-irradiated interstellar ice analog at low temperatures

Shogo Tachibana,[1]* Akira Kouchi,[2] Tetsuya Hama,[2] Yasuhiro Oba,[2] Laurette Piani,[1†] Iyo Sugawara,[1] Yukiko Endo,[1] Hiroshi Hidaka,[2] Yuki Kimura,[2] Ken-ichiro Murata,[2] Hisayoshi Yurimoto,[1,3] Naoki Watanabe[2]

Interstellar ice is believed to be a cradle of complex organic compounds, commonly found within icy comets and interstellar clouds, in association with ultraviolet (UV) irradiation and subsequent warming. We found that UV-irradiated amorphous ices composed of H_2O, CH_3OH, and NH_3 and of pure H_2O behave like liquids over the temperature ranges of 65 to 150 kelvin and 50 to 140 kelvin, respectively. This low-viscosity liquid-like ice may enhance the formation of organic compounds including prebiotic molecules and the accretion of icy dust to form icy planetesimals under certain interstellar conditions.

INTRODUCTION

Water-dominated ice is the most abundant solid component of dense molecular clouds and the outer cold part of protoplanetary disks (*1*) and must have played a critical role in the formation of gas and icy giants in the early solar system as a dominant component of their building blocks. Remnants of icy planetesimals (small bodies formed before planets in the early solar system) are now known as comets. Complex organic materials, including prebiotic molecules, have been observed in comets (*2*–*4*) and found in extraterrestrial materials such as returned cometary particles, interplanetary dust particles, carbonaceous micrometeorites, and chondrites (*5*–*8*). Ice and organic matter preserved in small planetesimals could have been a source of Earth's ocean and life (*9*), respectively. Consequently, understanding their formation and evolution in the solar system is one of the main scientific objectives of ongoing asteroidal sample-return missions (*10*, *11*).

Ultraviolet (UV) photon irradiation of amorphous H_2O-dominated ice in molecular clouds and/or in the outer part of protoplanetary disks may play a key role in synthesizing complex organic matter before the formation of cold planetesimals (*12*, *13*). As an example, a recent experimental study has shown that ribose, a major constituent of RNA, and related sugars can be synthesized by UV irradiation of an interstellar amorphous ice analog composed of H_2O, CH_3OH, and NH_3 at 78 K (*14*). Therefore, this process is critical to understanding the formation and evolution processes of ice and organic matter and their material properties as building blocks of outer solar system bodies and as a source of volatiles and ingredients of life delivered to the inner solar system. Here, we perform low-temperature photolysis experiments on an interstellar amorphous ice analog to understand the physical and chemical properties of interstellar ice.

RESULTS AND DISCUSSION

Mixtures of H_2O, CH_3OH, and NH_3 gases with molecular ratios of $H_2O/CH_3OH/NH_3$ (10–2:1:1) were deposited on a gold-coated copper substrate at 10 to 15 K with simultaneous UV photon irradiation in the low-temperature photolysis apparatus PICACHU (Photochemistry in Interstellar Cloud for Astro-Chronicle in Hokkaido University) (fig. S1 and table S1) (*15*). The gas deposition and UV photon fluxes were ~3.0×10^{14} to 5.9×10^{14} molecules cm^{-2} s^{-1} and ~1.0×10^{14} to 1.2×10^{14} photons cm^{-2} s^{-1}, respectively. Gas deposition, UV irradiation, and cooling of the substrate were stopped once the deposited amorphous ice had reached a thickness of several micrometers. The ice was observed in situ by an optical microscope during warm-up. In situ infrared reflectance spectra of similar amorphous ice have been acquired using another low-temperature photolysis apparatus [SAMRAI (setup for analysis of molecular and radical reactions of astrochemical interest)] (*16*). For comparison, experiments without UV irradiation were also performed.

The UV-irradiated ice with a smooth surface cracked at ~60 K like a brittle solid but started bubbling at ~65 K (the transition from solid-to-liquid–type cavitation). The bubbles were typically several to several tens of micrometers in radius (Fig. 1, figs. S2 and S3, and movie S1). The bubbling continued up to ~150 K, when the ice crystallized. This bubbling demonstrates that the UV-irradiated vapor-deposited amorphous ice changed into a liquid-like viscous material at temperatures in the range of 65 to 150 K, which is below its crystallization temperature. The ice sublimated at ~180 K to leave refractory organics with traces of bubbles (*15*). The number of bubbles depended on the ice composition, that is, fewer bubbles were observed for ice with higher H_2O contents. The bubbling behavior was observed only for the UV-irradiated ice not for the nonirradiated ice that formed from the same gas composition, which left no residual organics after sublimation.

The dominant gas species sublimated from the ice during bubbling was H_2, and spikes corresponding to H_2 were observed with quadrupole mass spectroscopy during the bubbling phase (Fig. 2A). Infrared spectroscopy of the UV-irradiated ice showed a notable H_2 feature in water-rich ice (*17*), which was not observed for the nonirradiated ice (Fig. 2B). The H_2 absorption feature disappeared at 140 to 150 K, which is the crystallization temperature of amorphous ice (fig. S4). These observations indicate that bubbling was caused by H_2 molecules formed by the photolysis of deposited molecules. The infrared spectrum of the UV-irradiated ice also showed that the peaks related solely to CH_3OH almost disappeared and that the peak of NH_3 at ~1100 cm^{-1} was lowered compared to the nonirradiated ice deposit (Fig. 2B), suggesting that hydrogen dissociated from CH_3OH and NH_3 (*18*, *19*) is the dominant source of bubbles. This is also supported by the observation that the number of bubbles decreased with increasing H_2O content in the ice.

[1]Department of Natural History Sciences, Hokkaido University, Sapporo, Hokkaido 060-0810, Japan. [2]Institute of Low Temperature Science, Hokkaido University, Sapporo, Hokkaido 060-0819, Japan. [3]Japan Aerospace Exploration Agency, Sagamihara, Kanagawa 252-5210, Japan.
*Corresponding author. Email: tachi@ep.sci.hokudai.ac.jp
†Present address: Centre de Recherches Pétrographiques et Géochimiques, 15 rue Notre Dame des Pauvres, 54500 Vandoeuvre-lès-Nancy, France.

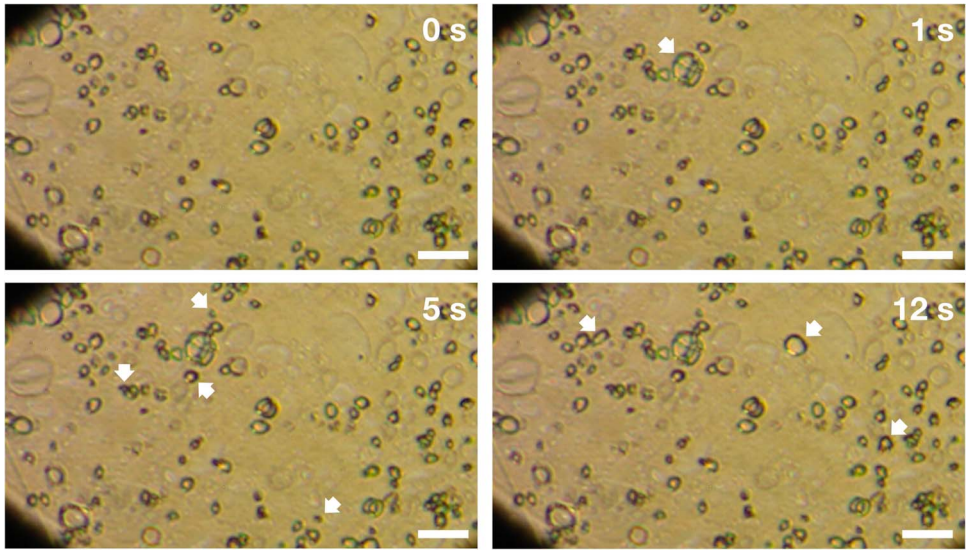

Fig. 1. Bubbles observed by an optical microscope (Nikon CM-10L) at 128 to 129 K in UV-irradiated amorphous H_2O–CH_3OH–NH_3 ice ($H_2O/CH_3OH/NH_3$, 5:1:1). The elapsed time from the first frame (0 s) (upper left) is shown in each figure, and newly exploded bubbles are indicated by arrows. Bubble growth occurred within a few to several seconds. Scale bars, 200 μm.

Similar hydrogen outbursts have been reported for proton-irradiated H_2O–NH_3 ice at 120 K (*20*), and we also confirmed that bubbling occurs for UV-irradiated H_2O–NH_3 ice at <120 K. Furthermore, we observed no bubbling in the nonirradiated H_2O–CH_3OH–NH_3 ice deposited with Ar or CO, which should exist in the gas phase at >80 K. This suggests that the bubbling does not occur solely due to the presence of volatile species in the amorphous ice.

The viscosity of the liquid-like amorphous ice was estimated from in situ microscopic observations of bubble growth (see Materials and Methods for details and fig. S3). The estimated viscosities at ~88 and ~112 K are ~4×10^2 to 7×10^2 Pa·s, much lower than the viscosity at the glass transition temperature (10^{12} Pa·s).

The observed liquid-like behavior cannot be explained by freezing point depression in the H_2O–CH_3OH–NH_3 ternary system (*21*). To confirm whether or not the liquid-like behavior is a characteristic property of the UV-irradiated H_2O-dominated amorphous ice, we used a low-temperature ultrahigh-vacuum transmission electron microscope (TEM) for in situ morphological observations of UV-irradiated amorphous water ice, where we focused on the morphological change of amorphous ice instead of bubbling. Islands of crystalline water ice (Ic) of several tens of nanometers in size were amorphized by UV irradiation at 10 K for 10 to 60 min, long enough for complete amorphization (fig. S5) (*22*). The shapes of the islands of amorphous water ice did not change up to 50 K, but at >50 K, we found clear morphological changes for the amorphous ice irradiated longer than 30 min. With increasing temperature, the heights of the islands decreased while their area increased, like squashed liquid droplets (Fig. 3A). The squashed islands finally overlapped and crystallized at ~140 K. Such a morphological change was not observed for either the water ice islands amorphized at 10 K with UV irradiation for 10 min or the crystalline water ice islands (Fig. 3C and fig. S6). Thus, we conclude that the morphological change in the islands of amorphous water ice at 50 to 140 K is spreading due to wetting, induced by liquefaction (or fluidization). Because the spreading behavior was not observed for the ice amorphized with UV irradiation for 10 min (~1.2×10^{16} photons cm^{-2}) but was observed in the case of irradiation for 30 min, the critical dose is about 2×10^{16} to 3×10^{16} photons cm^{-2} (a photon/molecule ratio of ~0.3). The viscosity of the UV-irradiated amorphous water ice at 60 K was estimated to be 4×10^7 Pa·s from the morphological change of the ice island (see Materials and Methods for details) (Fig. 3B). This viscosity is higher than that of UV-irradiated amorphous H_2O–CH_3OH–NH_3 ice but is still five orders of magnitude smaller than the viscosity at the glass transition temperature.

In the context of viscosity, we conclude that the UV-irradiated interstellar ice analog transformed into a liquid-like material below its crystallization temperature. The ice began to behave like liquid at 50 to 65 K, which is consistent with the temperature range (38 to 68 K) of the transition from high-density amorphous solid water (HD-ASW) (1.1 g cm^{-3}) deposited at 15 K to low-density ASW (LD-ASW) (0.94 g cm^{-3}) (fig. S7) (*23*, *24*). The high-to-low transition of ASW suggests that rearrangement of the hydrogen bond network occurs in the amorphous structure at 38 to 68 K. We speculate that the hydrogen bond rearrangement is enhanced by UV photolysis, possibly through breaking the hydrogen bond network and creating defects and/or radicals, which lowers the viscosity due to an increase in nonbridging atoms and molecules. Thus, we note that this liquid-like behavior should be regarded as a transient state during bond rearrangement.

The low-temperature liquid-like UV-irradiated interstellar ice could be an effective reaction medium for organic synthesis in low-temperature UV-illuminated environments in space, given the high mobility of molecules and radicals in low-viscosity media. Prebiotic or related molecules that formed in similar photochemical experiments (*25*–*27*) may have been synthesized through reactions in liquid-like media. The effective formation of ribose in organic residues synthesized from UV-irradiated ice at 78 K (*14*) might also be related to the appearance of a liquid-like medium, because the ice composition is the same as in the present study.

The UV flux in our experiments was 10^{13} to 10^{14} photons cm^{-2} s^{-1}, which is much higher than the flux within dense molecular clouds (~10^3 to 10^4 photons cm^{-2} s^{-1}), higher than the present interstellar UV flux (~10^8 photons cm^{-2} s^{-1}) and the flux in the uppermost layer of protoplanetary disks irradiated by a central star (~10^{11} photons cm^{-2} s^{-1}), and comparable to the flux at the uppermost layer of protoplanetary disks

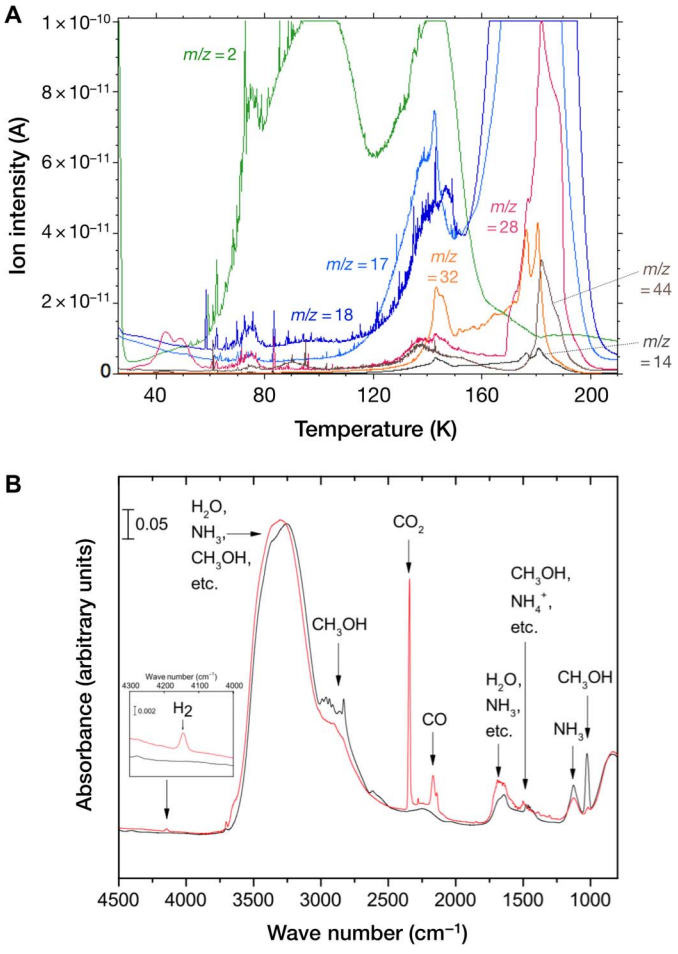

Fig. 2. Sublimated gases from UV-irradiated interstellar ice analog and its infrared absorption feature. (**A**) Quadrupole mass spectrometer signals of gas species sublimated from the UV-irradiated amorphous H_2O–CH_3OH–NH_3 ice during warm-up. The ion intensities are saturated at 1×10^{-10} A for mass/charge ratios (m/z) = 2, 17, and 18. H_2 signal spikes (m/z = 2) were observed at ~60 to 140 K. (**B**) Infrared spectra of the UV-irradiated (red curve) and non–UV-irradiated (black curve) H_2O–CH_3OH–NH_3 ices at 10 K. The inset shows enlarged spectra of the same samples at 4000 to 4300 cm^{-1}, where the H_2 peak in water-rich ice appeared for the UV-irradiated ice.

irradiated by external stars in a star cluster (~10^{11} to 10^{15} photons cm^{-2} s^{-1}) (*28*). The UV-irradiated water-rich ice behaved like a liquid in the case of an irradiation dose higher than 2×10^{16} to 3×10^{16} photons cm^{-2}. If the photon dose is crucial for the liquid-like behavior, then UV irradiation over 10^5 to 10^6 years is required inside dense molecular clouds, whereas a short irradiation (less than a day) is enough at the surface of protoplanetary disks in a star cluster. The photon flux may also be a key factor in the liquid-like behavior because the appearance of the transient low-viscosity state may depend on the lifetime of the radicals in the amorphous ice. If this is the case, then the liquid-like ice would not appear in dense molecular clouds but at the photoilluminated cold outer part of protoplanetary disks in a star cluster. In either case, at the outer part of protoplanetary disks, illumination from sibling stars can promote the synthesis of prebiotic molecules in low-viscosity reaction media if the temperature of the ice during the UV irradiation is low enough for the accumulation of defects and/or radicals.

The liquid-like ice appears as a transient state during the relaxation of photoirradiated ice at certain temperatures. Nevertheless, the liquid-like ice may also play an important role in the accretion of ice-coated dust in protoplanetary disks because it can dissipate the energy of dust collisions more effectively, via viscous dissipation, compared to brittle solid ice. Although a further discussion of the dust collision rate and the time span of the liquid-like transient state under interstellar conditions is desirable, the effective accretion of ice-coated dust in outer protoplanetary disks might result in the rapid formation of planets, as suggested for a protoplanetary disk around a very young T Tauri star, HL Tau, in a giant molecular cloud by the Atacama Large Millimeter/submillimeter Array (ALMA) (*29*).

MATERIALS AND METHODS

In situ observation of bubbling

The UV-irradiated H_2O–CH_3OH–NH_3 amorphous ice was produced with the PICACHU apparatus following the protocol reported in the study by Piani *et al.* (*15*), but the position of the glass window of the vacuum chamber was lowered for in situ microscopic observation of the ice during warm-up (fig. S1). The experimental conditions are summarized in table S1. The PICACHU apparatus can deposit mixed gas onto three faces of a cuboid substrate holder through capillary plates, and the gold-coated copper substrate attached to one of the faces of the substrate holder was observed using an optical microscope (Nikon CM-10L) with a magnification of ×10 (fig. S1). For run 081, a high-speed optical microscope (Keyence VW-9000) with a long-distance zoom lens (VW-Z2) was used for detailed observation of bubbles. In runs 037 and 052 without UV irradiation, we mixed Ar or CO with the H_2O–CH_3OH–NH_3 gas (H_2O/CH_3OH/NH_3/Ar, 5:1:1:1; H_2O/CH_3OH/NH_3/CO, 4:0:2:1) (table S1).

An order-of-magnitude estimate of the viscosity was made from the expansion of bubbles (fig. S2). The time-dependent bubble expansion was given by

$$4\,\eta\,\frac{\dot{R}}{R} = P_{in} - P_{ice} - \frac{2\gamma}{R} \quad (1)$$

where η is the viscosity, R is the bubble radius, P_{in} is the gas pressure inside a bubble, P_{ice} is the pressure of ice surrounding the bubble, and γ is the surface tension (*30*). We simply assumed that P_{in} is constant during the early growth phase of the bubble because the diffusion of H_2 molecules in water ice is quite rapid (10^{-4} cm^2 s^{-1} at 60 K) (*31*). The expansion of the bubble was then expressed by

$$R = \frac{2\gamma}{P_{in} - P_{ice}}\left(\exp\left(\frac{P_{in} - P_{ice}}{4\eta}t\right)\left(\frac{2\gamma}{P_{in} - P_{ice}}R_0 - 1\right) + 1\right) \quad (2)$$

where R_0 is the radius of the initial nucleus. We can obtain $2\gamma/(P_{in} - P_{ice})$ and $(P_{in} - P_{ice})/4\eta$ by fitting the bubble growth (fig. S3), and therefore, $2\eta/\gamma$. With γ of 0.07 N m^{-1} (*32*), the viscosity of the UV-irradiated H_2O–CH_3OH–NH_3 amorphous ice was estimated to be ~4×10^2 to 7×10^2 Pa·s at 88 and 112 K.

Infrared reflectance spectroscopy

The infrared spectrum of the UV-irradiated ice analog (Fig. 2B) was obtained with a reflection-absorption–type Fourier transform infrared

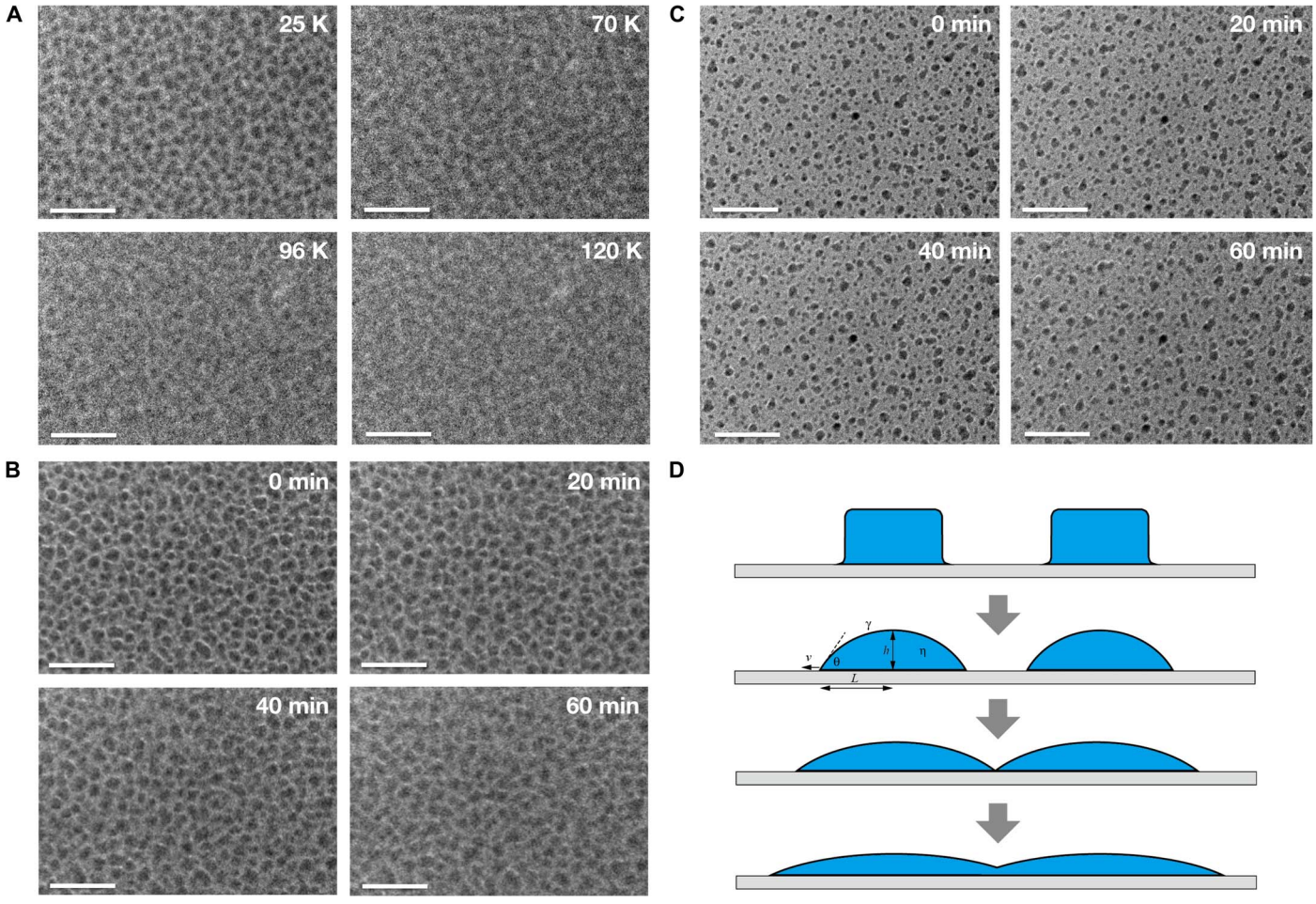

Fig. 3. In situ TEM observation of UV-irradiated amorphous water ice and ice Ic. (**A**) TEM images of amorphous water ice islands, irradiated by UV at 10 K for 50 min, at different temperatures during warm-up (see Materials and Methods and fig. S5 for details about the synthesis of amorphous ice islands). Image contrast shows differences in thickness, and the darker parts represent thicker ice (that is, islands of amorphous ice). The contrast became blurred with increased temperature. Note that the images at different temperatures were taken in different regions of the samples. (**B**) Wetting process of amorphous water ice (UV irradiation for 50 min at 10 K) at 60 K. The same sample area was observed for over 60 min, and the contrast became blurred with time. (**C**) Ice Ic observed at 60 K for 60 min without UV irradiation. Islands of ice Ic were made from an ASW film deposited at 6 K by heating at 145 K for 10 min (see Materials and Methods and fig. S5). Observations were made at the same position in the sample. Scale bars, 500 nm (A to C). (**D**) Schematic of the wetting process.

spectrometer with a resolution of 4 cm^{-1} equipped with the SAMRAI apparatus, following the protocol reported in the study by Oba *et al.* (*16*). A H_2O–CH_3OH–NH_3 gas mixture (5:1:1) was deposited on an aluminum substrate at 10 K through a capillary plate at a total gas flow of ~10^{13} molecules cm^{-2} s^{-1}. The samples were exposed to UV photons throughout the deposition period of 18.5 hours. The UV photon flux was ~7 × 10^{13} photons cm^{-2} s^{-1}. After simultaneous gas deposition and photon irradiation, the substrate was warmed to room temperature at a rate of 1 K min^{-1}. For comparison, the non–UV-irradiated ice was produced by the deposition of the same gas mixture at the same deposition rate for 16.5 hours. The experimental conditions with SAMRAI are also listed in table S1. The presence of H_2 was confirmed only in the UV-irradiated sample (Fig. 2B). The column density of H_2 was calculated using the band strength of the peak at 4145 cm^{-1}, 9 × 10^{-20} cm $molecule^{-1}$ (*17*). The column density of H_2 decreased with increasing substrate temperature (fig. S4), and the decrease of the column density was enhanced at >60 K probably due to the transition of the ice to a liquid-like material.

Transmission electron microscope

For the in situ deposition and observation of the UV-irradiated amorphous water ice, we developed a 200-kV ultrahigh-vacuum TEM (JEOL JEM-2100VL) following the study by Kondo *et al.* (*33*). A column of the TEM was evacuated with five ion pumps, two Ti sublimation pumps, and two turbomolecular pumps. The pressure of the specimen chamber was 1 × 10^{-6} Pa, as measured with an ionization gauge. The pressure near the specimen was expected to be lower than 1 × 10^{-6} Pa because the specimen is surrounded by a liquid nitrogen shroud. A 5-nm-thick amorphous Si film with a single-crystalline Si grid (SiMPore Inc.) was used as a substrate for sample deposition, which was cooled using a liquid He cooling holder (Gatan ULTST). Two of the three ports directed at the specimen surface with an incident angle of 55° were used for a Ti gas inlet tube (inner diameter, 0.4 mm) and UV irradiation. UV rays from a 30-W D_2 lamp with a MgF_2 window (Hamamatsu L7293) were collimated using a mirror-finished pure Al collimator with an estimated flux of (2 ± 1) × 10^{13} photons cm^{-2} s^{-1}.

Because a uniform film of amorphous water ice was not adequate for the observation of morphological changes in the ice, we made the

islands of amorphous ice as follows (fig. S5). A uniform film of amorphous water ice was first deposited with a deposition rate of 5 nm min^{-1} at 6 to 8 K. The thickness of the ice deposit was 25 ± 5 nm [(8.4 ± 1.7) × 10^{16} H_2O cm^{-2}]. The film was warmed up to 145 K to form the islands of crystalline water ice (ice Ic) (*34*). The islands of ice Ic were then cooled to 10 K and irradiated with UV rays for 30 min. Ice Ic was amorphized within 1 min (*22*), and with further UV irradiation, the height of the islands decreased, and their area increased (fig. S5). After UV irradiation, the sample was heated at a manually controlled rate of ~5 K min^{-1} to observe the morphological change of the islands (Fig. 3A). To avoid electron beam damage to the sample, low-magnification images (×50,000) were recorded using a charge-coupled device (CCD) camera (Gatan ES500W) with an accelerating voltage of 80 kV, which resulted in an electron beam density of ~6 × 10^{-3} electrons $Å^{-2}$ at the sample location. Furthermore, observations at different temperatures were made at different sites on the sample. For continuous observation of the morphological change in the islands at 60 K (Fig. 3B), the islands of amorphous water ice were warmed up to 60 K over ~30 min, and a low–electron dose imaging technique was applied to obtain images. The camera length of TEM was calibrated using the edge of a Si grid. Along with in situ observation, we measured the *d* space of the main halo of the amorphous ice in the electron diffraction patterns to obtain structural information on the amorphous water ice. For comparison, the same observations were also made on the islands of ice Ic.

We observed morphological changes in UV-irradiated amorphous water ice islands (Fig. 3B) but not in crystalline water ice islands (Fig. 3C), as suggested by the frequency distribution of the relative number of transmitted electrons deduced from the intensity at each pixel of the CCD camera (fig. S6). Because the number of transmitted electrons increases with decreasing sample thickness, the peak shift to higher transmittance seen in the UV-irradiated amorphous water ice islands (fig. S6) qualitatively corresponded to the lowering of the island height with time. We also saw sharpening of the peak, indicating that the island height becomes more uniform with time. Because we did not see any significant change in the frequency distribution for the nonirradiated crystalline water ice islands (fig. S6), we can conclude that the electron beam does not affect the in situ TEM observations. These series of observations led us to conclude that the spreading of the UV-irradiated amorphous water ice due to wetting occurs at 60 K.

The order-of-magnitude estimate of the viscosity of UV-irradiated amorphous water ice was made from the morphological change of the islands at 60 K (Fig. 3B). The viscosity η was calculated as follows (*35*)

$$\eta \sim \theta^3 \gamma / v \qquad (3)$$

where θ is the contact angle, γ is the surface tension, and *v* is the spreading velocity. The contact angle θ of ~0.38 was obtained from the height and radius of islands. The height of the island was estimated from the sublimation time scale of the ice at 160 K. With θ = ~0.38 and *v* = ~0.1 nm s^{-1} from in situ observations and γ = 0.07 N m^{-1} (*32*), we obtained η = ~4 × 10^7 Pa·s. This viscosity was four to five orders of magnitude smaller than that at the glass transition temperature (10^{12} Pa·s), indicating that the UV-irradiated amorphous water ice behaves like a viscous liquid.

The temperature dependence of the *d* space of the halo of UV-irradiated amorphous water ice is shown in fig. S7. The *d* spaces of UV-irradiated amorphous water ices were slightly smaller than those of HD-ASW at <40 K. The *d* space increased with temperature and approached that of LD-ASW at ~140 K. In the temperature range where the liquid-like behavior was observed, the *d* space of UV-irradiated amorphous water ice was smaller than that of LD-ASW, suggesting that the UV-irradiated amorphous water ice has a denser structure than HD-ASW or LD-ASW (fig. S7).

SUPPLEMENTARY MATERIALS

Supplementary material for this article is available at http://advances.sciencemag.org/cgi/content/full/3/9/eaao2538/DC1

fig. S1. Setup of the PICACHU apparatus for in situ observations of bubbles.
fig. S2. Successive images of bubble growth (within the area indicated by a dotted circle) at 88 K (run 081) observed by a high-speed optical microscope (Keyence VW-9000) with a long-distance zoom lens (VW-Z2).
fig. S3. Growth of bubbles at 88 K (run 081) and 112 K (run 056).
fig. S4. Change in column density of H_2 molecules in the UV-irradiated H_2O–CH_3OH–NH_3 ice as substrate temperature increases at a rate of 1 K min^{-1}.
fig. S5. Formation procedure of amorphous ice islands by UV irradiation of ice Ic with low-magnification TEM images and electron diffraction patterns of the ice.
fig. S6. Temporal change in the frequency distributions of the relative number of transmitted electrons in TEM images during 60 min of observation of UV-irradiated amorphous water-rich ice (left) and nonirradiated crystalline water-rich ice (right) at 60 K.
fig. S7. Temperature dependence of the *d* space of the main halo of electron diffraction patterns of UV-irradiated amorphous water ice.
table S1. Experimental conditions and summary of bubbling occurrence (y, yes; n, no).
movie S1. Bubbling of the UV-irradiated amorphous H_2O–CH_3OH–NH_3 ice (H_2O/CH_3OH/NH_3, 5:1:1) at 128 to 129 K.
Reference (*36*)

REFERENCES AND NOTES

1. R. M. E. Mastrapa, W. M. Rundy, M. S. Gudipati, *Amorphous and Crystalline H_2O-ice*, vol. 356 of *The Science of Solar System Ices (Astrophysics and Space Science Library)*, M. S. Gudipati, J. Castillo-Rogez, Eds. (Springer, 2013), pp. 371–408.
2. F. Capaccioni, A. Coradini, G. Filacchione, S. Erard, G. Arnold, P. Drossart, M. C. De Sanctis, D. Bockelee-Morvan, M. T. Capria, F. Tosi, C. Leyrat, B. Schmitt, E. Quirico, P. Cerroni, V. Mennella, A. Raponi, M. Ciarniello, T. McCord, L. Moroz, E. Palomba, E. Ammannito, M. A. Barucci, G. Bellucci, J. Benkhoff, J. P. Bibring, A. Blanco, M. Blecka, R. Carlson, U. Carsenty, L. Colangeli, M. Combes, M. Combi, J. Crovisier, T. Encrenaz, C. Federico, U. Fink, S. Fonti, W. H. Ip, P. Irwin, R. Jaumann, E. Kuehrt, Y. Langevin, G. Magni, S. Mottola, V. Orofino, P. Palumbo, G. Piccioni, U. Schade, F. Taylor, D. Tiphene, G. P. Tozzi, P. Beck, N. Biver, L. Bonal, J.-P. Combe, D. Despan, E. Flamini, S. Fornasier, A. Frigeri, D. Grassi, M. Gudipati, A. Longobardo, K. Markus, F. Merlin, R. Orosei, G. Rinaldi, K. Stephan, M. Cartacci, A. Cicchetti, S. Giuppi, Y. Hello, F. Henry, S. Jacquinod, R. Noschese, G. Peter, R. Politi, J. M. Reess, A. Semery, The organic-rich surface of comet 67P/Churyumov-Gerasimenko as seen by VIRTIS/Rosetta. *Science* **347**, aaa0628 (2015).
3. N. Fray, A. Bardyn, H. Cottin, K. Altwegg, D. Baklouti, C. Briois, L. Colangeli, C. Engrand, H. Fischer, A. Glasmachers, E. Grün, G. Haerendel, H. Henkel, H. Höfner, K. Hornung, E. K. Jessberger, A. Koch, H. Krüger, Y. Langevin, H. Lehto, K. Lehto, L. Le Roy, S. Merouane, P. Modica, F. R. Orthous-Daunay, J. Paquette, F. Raulin, J. Rynö, R. Schulz, J. Silén, S. Siljeström, W. Steiger, O. Stenzel, T. Stephan, L. Thirkell, R. Thomas, K. Torkar, K. Varmuza, K. P. Wanczek, B. Zaprudin, J. Kissel, M. Hilchenbach, High-molecular-weight organic matter in the particles of comet 67P/Churyumov–Gerasimenko. *Nature* **538**, 72–74 (2016).
4. J. Kissel, R. Z. Sagdeev, J. L. Bertaux, V. N. Angarov, J. Audouze, J. E. Blamont, K. Büchler, E. N. Evlanov, H. Fechtig, M. N. Fomenkova, H. von Hoerner, N. A. Inogamov, V. N. Khromov, W. Knabe, F. R. Krueger, Y. Langevin, V. B. Leonas, A. C. Levasseurregourd, G. G. Managadze, S. N. Podkolzin, V. D. Shapiro, S. R. Tabaldyev, B. V. Zubkov, Composition of comet Halley dust particles from Vega observations. *Nature* **321**, 280–282 (1986).
5. S. A. Sandford, J. Aléon, C. M. O.'D. Alexander, T. Araki, S. Bajt, G. A. Baratta, J. Borg, J. P. Bradley, D. E. Brownlee, J. R. Brucato, M. J. Burchell, H. Busemann, A. Butterworth, S. J. Clemett, G. Cody, L. Colangeli, G. Cooper, L. D'Hendecourt, Z. Djouadi, J. P. Dworkin, G. Ferrini, H. Fleckenstein, G. J. Flynn, I. A. Franchi, M. Fries, M. K. Gilles, D. P. Glavin, M. Gounelle, F. Grossemy, C. Jacobsen, L. P. Keller, A. L. D. Kilcoyne, J. Leitner, G. Matrajt, A. Meibom, V. Mennella, S. Mostefaoui, L. R. Nittler, M. E. Palumbo, D. A. Papanastassiou, F. Robert, A. Rotundi, C. J. Snead, M. K. Spencer, F. J. Stadermann, A. Steele, T. Stephan, P. Tsou, T. Tyliszczak, A. J. Westphal, S. Wirick, B. Wopenka, H. Yabuta, R. N. Zare,

M. E. Zolensky, Organics captured from comet 81P/Wild 2 by the Stardust spacecraft. *Science* **314**, 1720–1724 (2006).
6. J. Duprat, E. Dobrică, C. Engrand, J. Aléon, Y. Marrocchi, S. Mostefaoui, A. Meibom, H. Leroux, J.-N. Rouzaud, M. Gounelle, F. Robert, Extreme deuterium excesses in ultracarbonaceous micrometeorites from central Antarctic snow. *Science* **328**, 742–745 (2010).
7. T. Noguchi, H. Yabuta, S. Itoh, N. Sakamoto, T. Mitsunari, A. Okubo, R. Okazaki, T. Nakamura, S. Tachibana, K. Terada, M. Ebihara, N. Imae, M. Kimura, H. Nagahara, Variation of mineralogy and organic material during the early stages of aqueous activity recorded in Antarctic micrometeorites. *Geochim. Cosmochim. Acta* **208**, 119–144 (2017).
8. C. M. O'D. Alexander, G. D. Cody, B. T. De Gregorio, L. R. Nittler, R. M. Stroud, The nature, origin and modification of insoluble organic matter in chondrites, the major source of Earth's C and N. *Chemie der Erde* **77**, 227–256 (2017).
9. B. Marty, The origins and concentrations of water, carbon, nitrogen and noble gases on Earth. *Earth Planet. Sci. Lett.* **313–314**, 56–66 (2012).
10. S. Tachibana, M. Abe, M. Arakawa, M. Fujimoto, Y. Iijima, M. Ishiguro, K. Kitazato, N. Kobayashi, N. Namiki, T. Okada, R. Okazaki, H. Sawada, S. Sugita, Y. Takano, S. Tanaka, S. Watanabe, M. Yoshikawa, H. Kuninaka; The Hayabusa2 Project Team, Hayabusa2: Scientific importance of samples returned from C-type near-Earth asteroid (162173) 1999 JU_3. *Geochem. J.* **48**, 571–587 (2014).
11. D. S. Lauretta, A. E. Bartels, M. A. Barucci, E. B. Bierhaus, R. P. Binzel, W. F. Bottke, H. Campins, S. R. Chesley, B. C. Clark, B. E. Clark, E. A. Cloutis, H. C. Connolly, M. K. Crombie, M. Delbó, J. P. Dworkin, J. P. Emery, D. P. Glavin, V. E. Hamilton, C. W. Hergenrother, C. L. Johnson, L. P. Keller, P. Michel, M. C. Nolan, S. A. Sandford, D. J. Scheeres, A. A. Simon, B. M. Sutter, D. Vokrouhlický, K. J. Walsh, The OSIRIS-REx target asteroid (101955) Bennu: Constraints on its physical, geological, and dynamical nature from astronomical observations. *Meteorit. Planet. Sci.* **50**, 834–849 (2015).
12. J. M. Greenberg, Making a comet nucleus. *Astron. Astrophys.* **330**, 375–380 (1998).
13. F. J. Ciesla, S. A. Sandford, Organic synthesis via irradiation and warming of ice grains in the solar nebula. *Science* **336**, 452–454 (2012).
14. C. Meinert, I. Myrgorodska, P. De Marcellus, T. Buhse, L. Nahon, S. V. Hoffmann, L. L. S. d'Hendecourt, U. J. Meierhenrich, Ribose and related sugars from ultraviolet irradiation of interstellar ice analogs. *Science* **352**, 208–212 (2016).
15. L. Piani, S. Tachibana, T. Hama, H. Tanaka, Y. Endo, I. Sugawara, L. Dessimoulie, Y. Kimura, A. Miyake, J. Matsuno, A. Tsuchiyama, K. Fujita, S. Nakatsubo, H. Fukushi, S. Mori, T. Chigai, H. Yurimoto, A. Kouchi, Evolution of morphological and physical properties of laboratory interstellar organic residues with ultraviolet irradiation. *Astrophys. J.* **837**, 35–45 (2017).
16. Y. Oba, Y. Takano, N. Watanabe, A. Kouchi, Deuterium fractionation during amino acid formation by photolysis of interstellar ice analogs containing deuterated methanol. *Astrophys. J. Lett.* **827**, L18 (2016).
17. S. A. Sandford, L. J. Allamandola, H_2 in interstellar and extragalactic ices—Infrared characteristics, ultraviolet production, and implications. *Astrophys. J.* **409**, L65–L68 (1993).
18. T. Hama, M. Yokoyama, A. Yabushita, M. Kawasaki, Translational and internal states of hydrogen molecules produced from the ultraviolet photodissociation of amorphous solid methanol. *J. Chem. Phys.* **130**, 164505 (2009).
19. P. A. Gerakines, W. A. Schutte, P. Ehrenfreund, Ultraviolet processing of interstellar ice analogs. I. Pure ices. *Astron. Astrophys.* **312**, 289–305 (1996).
20. M. J. Loeffler, R. A. Baragiola, Blistering and explosive desorption of irradiated ammonia-water mixtures. *Astrophys. J.* **744**, 102–108 (2012).
21. J. S. Kargel, thesis, University of Arizona (1990).
22. A. Kouchi, T. Kuroda, Amorphization of cubic ice by ultraviolet irradiation. *Nature* **344**, 134–135 (1990).
23. P. Jenniskens, D. F. Blake, Structural transitions in amorphous water ice and astrophysical implications. *Science* **265**, 753–756 (1994).
24. P. Jenniskens, D. F. Blake, M. A. Wilson, A. Pohorille, High-density amorphous ice, the frost on interstellar grains. *Astrophys. J.* **455**, 389–401 (1995).
25. R. Briggs, G. Ertem, J. Ferris, J. M. Greenberg, P. J. McCain, C. X. Mendoza-Gomez, W. Schutte, Comet Halley as an aggregate of interstellar dust and further evidence for the photochemical formation of organics in the interstellar medium. *Orig. Life Evol. Biosph.* **22**, 287–307 (1992).
26. G. M. Muñoz Caro, U. J. Meierhenrich, W. A. Schutte, B. Barbier, A. Arcones Segovia, H. Rosenbauer, W. H.-P. Thiemann, A. Brack, J. M. Greenberg, Amino acids from ultraviolet irradiation of interstellar ice analogues. *Nature* **416**, 403–406 (2002).
27. M. P. Bernstein, J. P. Dworkin, S. A. Sandford, G. W. Cooper, L. J. Allamandola, Racemic amino acids from the ultraviolet photolysis of interstellar ice analogues. *Nature* **416**, 401–403 (2002).
28. H. B. Throop, UV photolysis, organic molecules in young disks, and the origin of meteoritic amino acids. *Icarus* **212**, 885–895 (2011).
29. ALMA Partnership; C. L. Brogan, L. M. Pérez, T. R. Hunter, W. R. F. Dent, A. S. Hales, R. E. Hills, S. Corder, E. B. Fomalont, C. Vlahakis, Y. Asaki, D. Barkats, A. Hirota, J. A. Hodge, C. M. V. Impellizzeri, R. Kneissl, E. Liuzzo, R. Lucas, N. Marcelino, S. Matsushita, K. Nakanishi, N. Phillips, A. M. S. Richards, I. Toledo, R. Aladro, D. Broguiere, J. R. Cortes, P. C. Cortes, D. Espada, F. Galarza, D. Garcia-Appadoo, L. Guzman-Ramirez, E. M. Humphreys, T. Jung, S. Kameno, R. A. Laing, S. Leon, G. Marconi, A. Mignano, B. Nikolic, L.-A. Nyman, M. Radiszcz, A. Remijan, J. A. Rodón, T. Sawada, S. Takahashi, R. P. J. Tilanus, B. Vila Vilaro, L. C. Watson, T. Wiklind, E. Akiyama, E. Chapillon, I. de Gregorio-Monsalvo, J. Di Francesco, F. Gueth, A. Kawamura, C.-F. Lee, Q. Nguyen Luong, J. Mangum, V. Pietu, P. Sanhueza, K. Saigo, S. Takakuwa, C. Ubach, T. van Kempen, A. Wootten, A. Castro-Carrizo, H. Francke, J. Gallardo, J. Garcia, S. Gonzalez, T. Hill, T. Kaminski, Y. Kurono, H.-Y. Liu, C. Lopez, F. Morales, K. Plarre, G. Schieven, L. Testi, L. Videla, E. Villard, P. Andreani, J. E. Hibbard, K. Tatematsu, The 2014 ALMA long baseline campaign: First results from high angular resolution observations toward the HL Tau region. *Astrophys. J. Lett.* **808**, L3–L12 (2015).
30. A. A. Proussevich, D. L. Sahagian, A. T. Anderson, Dynamics of diffusive bubble growth in magmas: Isothermal case. *J. Geophys. Res.* **98**, 22283–22307 (1993).
31. H. L. Strauss, Z. Chen, C.-K. Loong, The diffusion of H_2 in hexagonal ice at low temperatures. *J. Chem. Phys.* **101**, 7177–7180 (1994).
32. V. F. Petrenko, R. W. Whitworth, *Physics of Ice* (Oxford Univ. Press, 1999).
33. Y. Kondo, K. Ohi, Y. Ishibashi, H. Hirano, Y. Harada, K. Takayanagi, Y. Tanishiro, K. Kobayashi, K. Yagi, Design and development of an ultrahigh vacuum high-resolution transmission electron microscope. *Ultramicroscopy* **35**, 111–118 (1991).
34. P. Jenniskens, D. F. Blake, Crystallization of amorphous water ice in the solar system. *Astrophys. J.* **473**, 1104–1113 (1996).
35. L. H. Tanner, The spreading of silicone oil drops on horizontal surfaces. *J. Phys. D Appl. Phys.* **12**, 1473–1484 (1979).
36. A. Kouchi, T. Hama, Y. Kimura, H. Hidaka, R. Escribano, N. Watanabe, Matrix sublimation method for the formation of high-density amorphous ice. *Chem. Phys. Lett.* **658**, 287–292 (2016).

Acknowledgments: We thank O. Yamamuro and M. Fukazawa for helpful comments and discussion, and S. Nakatsubo, K. Fujita, K. Sinbori, and M. Ikeda for help in the development of the ultrahigh-vacuum TEM. **Funding:** This work was supported by the Ministry of Education, Culture, Sports, Science, and Technology Grants-in-Aid for Scientific Research (KAKENHI; grant 25108002) and the Japan Society for the Promotion of Science (KAKENHI; grant 16H04072).
Author contributions: S.T. and A.K. designed and directed the study. I.S., Y.E., L.P., S.T., T.H., and A.K. performed the in situ observation of bubbling. Y.O. conducted the infrared spectroscopy. A.K., H.H., and Y.K. carried out the TEM observation. K.M., H.Y., and N.W. discussed the data. S.T., A.K., Y.O., and T.H. wrote the manuscript. All authors commented on the paper. **Competing interests:** The authors declare that they have no competing interests. **Data and materials availability:** All data needed to evaluate the conclusions in the paper are present in the paper and/or the Supplementary Materials. Additional data related to this paper may be requested from the authors.

Submitted 30 June 2017
Accepted 7 September 2017
Published 29 September 2017
10.1126/sciadv.aao2538

Citation: S. Tachibana, A. Kouchi, T. Hama, Y. Oba, L. Piani, I. Sugawara, Y. Endo, H. Hidaka, Y. Kimura, K. Murata, H. Yurimoto, N. Watanabe, Liquid-like behavior of UV-irradiated interstellar ice analog at low temperatures. *Sci. Adv.* **3**, eaao2538 (2017).